Active Carbon at High Temperature

Our initial reactor design required high temperatures, around 250° C, to be able to work in vapour phase. For starting with the study of the reaction catalysis, iron based catalysts were chosen (see *Chapter 3.4*). The decision to begin testing such catalysts was the fact that the active species used in biocatalysis for this reaction is an iron di-oxo specie [1, 2]. Another reason for choosing an iron catalyst lied on the fact that iron oxide based catalysts have dehydrogenating properties in the reaction of synthesis of styrene [3-7]. Several iron oxide catalysts were synthesized and tested. However no significant catalytic results were obtained.

Because of some reported evidences that the dehydrogenating active sites are located on a carbonaceous overlayer rather than on the oxide catalyst surface, we decided to test carbonaceous materials, as well. Thereafter, iron supported on carbon materials containing a metal loading of 5 % was prepared (see *Chapter 3.4*). Some changes comparing to previous experiments were observed. Since many new GC peaks were obtained, it was decided to carry out a structural determination analysis of the *unknown* compounds, based on the use of GC-MS and ^{1}H-NMR (*see Chapter 4.2*). The identification of aromatic FAEE was in good agreement with a reported aromatization of linoleic acid in batch reactor [8]., in which no definite structures were proposed. Analogously, palladium supported AC catalyst were prepared to study the effect of the supported metal.

In order to find out the component responsible of the catalytic activity (metallic phase, support or both), a blank experiment using carbon without iron was performed, resulting that active carbon presented a similar GC profile to that obtained with iron supported on active carbon. Therefore, a thorough study of active carbon and its relation to catalytic activity was required and became an important part of this work.

The obtaining of ethyl oleate as a product of hydrogenation turned out to be of special importance, because, in a way, it was another proof that dehydrogenation

was occurring. In some cases, hydrogenation products had such a high value of selectivity that it was a must to pose several questions. Where did this hydrogen come from? Were dehydrogenation products the only hydrogen source? Benzene hydrogenation was used as a *hydrogen capturer*, to remove part of the produced hydrogen. The results are discussed.

From the scientific bibliography we find that carbonaceous materials have been used in the dehydrogenation reaction of ethylbenzene [9-14]. Figueiredo et al. [15-20] and Schlögl et al. [21-26] played a key role in the study of the dehydrogenation activity of these materials. Besides its textural properties, active carbon exhibits a chemical structure as well. A component of these materials was reported to be carbon in a sp^2 hybridisation [27]. The surface functionality is mainly given by oxygen-containing groups, although an appreciable amount of other heteroatoms, such as hydrogen, nitrogen, sulphur or chlorine, may also be present. However, surface carbon-oxygen structures are by far the most important structures in influencing the surface behaviour of carbons. These surface groups cannot be treated as ordinary organic compounds though, since they interact differently in different environments. Their behaviour as combined structures depends on their location on the polyaromatic frame [27]

Regarding the feature responsible for the dehydrogenation activity, a suggested mechanism is that based on the red-ox reaction of carbonyl to hydroxyl groups coupled to the dehydrogenation reaction. In this case, oxygen-containing gas feed is added to regenerate the active phase [15, 26]. The influence of the surface chemistry of our material was studied by altering the functionality under an oxidative treatment, and results are discussed.

3.5.1 Experimental

The catalytic tests were performed at 240 °C with 0.055 and 0.11 μmol g_{cat}^{-1} s^{-1} using argon as inert carrier with a flow of 0.225 mL/s. The samples were diluted in ethanol before being analysed by GC.

Active carbon (AC) was used as a catalyst. An oxidative treatment was performed to AC (AC_{0h}) in order to study the effect of modifying the surface chemistry. This treatment consisted of oxidizing the carbons (0.8 g) under 5% O_2 in helium for 3 hours (AC_{3h}) and 11 hours (AC_{11h}) at 425 °C.

The catalysts were characterized by nitrogen physisorption using the BET method, elemental analysis, temperature-programmed desorption (TPD) coupled to mass spectrometry, scanning-electron microscopy and FTIR spectroscopy.

3.5.2 Results and Discussion

Characterization of active carbon

The influence of the functionality in the reactivity of ethyl linoleate was studied, in a first attempt, by the use of FTIR spectroscopy (Fig. 3.5.1). AC and AC_{3h} showed a weak band centred at 2300 cm^{-1}. It is difficult to assign a particular functionality to this band due to the limited number of bonds that absorb at this region [28]. However, previous studies proposed that carbon-oxygen bonds in ketenes [29-31] and surface C≡C triple bond stretches [32, 33] give bands around 2300 cm^{-1}. Recently, Guo et al. assigned this band to C≡O stretching vibration due to the enriched carbon dioxide atmosphere during the activation process [34]. This peak disappeared in the analysis performed to AC_{11h}. Nevertheless, two wide and weak

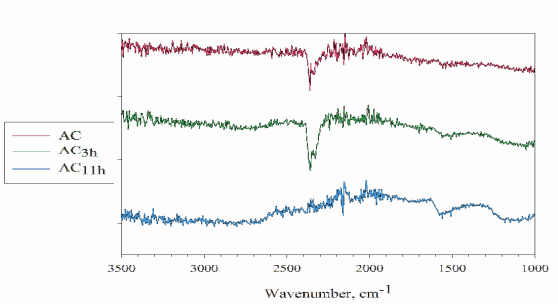

Figure 3.5.1 FTIR spectra of carbons.

absorption bands were detected at 1600 cm^{-1} and at 1150 cm^{-1}. The band at 1600 cm^{-1} is generally assigned to C=O stretching modes in groups, such as carboxylic acids, carboxylic anhydrides, lactones and quinones. The bands at 1150 cm^{-1} correspond to C-O stretches in functional groups, such as ethers, carboxylic acids, phenols, esters and epoxides [28, 32, 35]. The difficult interpretation of spectra is due to the fact that each functional group originates several bands, so that each band may include contribution of different groups. Moreover, the limit of detectability of this technique did not allow detecting clearly the functional groups of interest and forced the search of another methodology to evaluate the surface chemistry of the catalysts. FTIR can be applied only to highly oxidized carbons; otherwise the intensity of the bands is not sufficient [32]. As a rough guide, below about 3 per cent by weight, detection becomes relatively difficult; although it depends on some parameters, such as the nature of functional groups, the scanning speed, slit width, etc. [33].

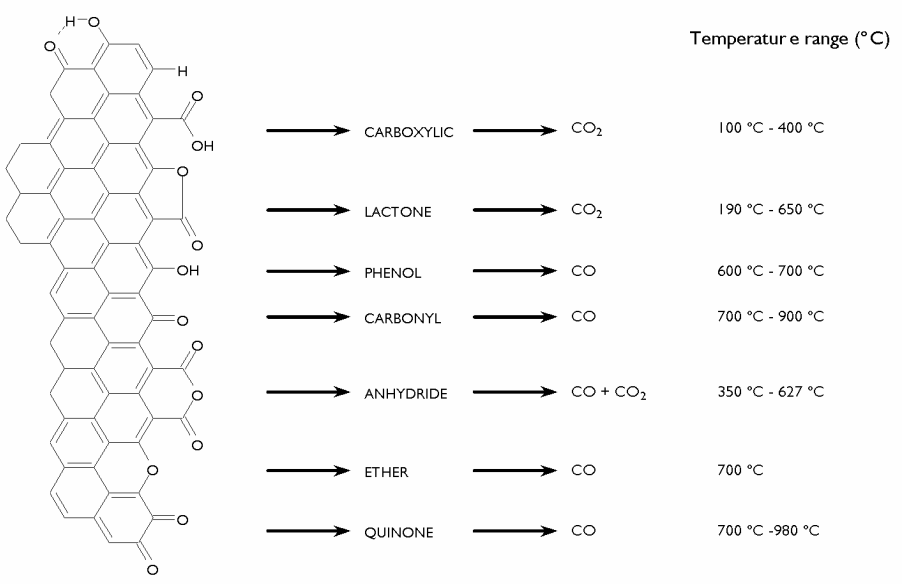

Figure 3.5.2 Surface groups and their decomposition gases at different temperatures [34].

A popular alternative to FTIR is the decomposition of surface oxygen-containing groups to CO and CO_2 at different temperatures. Although the assignment of TPD peaks to determine functional groups may depend on different factors, such as the

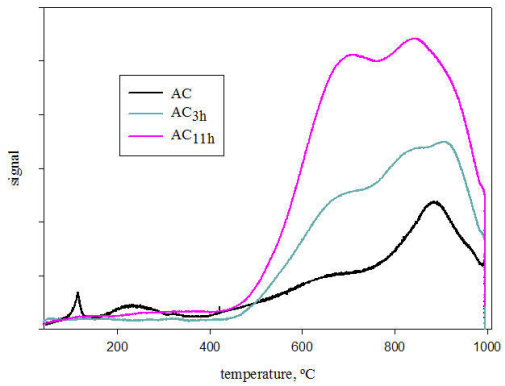

Figure 3.5.3 TPD profiles of carbons.

heating rate, the textural properties and the experimental system design [36-38], there are some well-established trends related to functionality (Fig. 3.5.2) [35]. Therefore CO_2 is eluted at lower temperatures, when carboxylic acids are present. At higher temperatures, CO_2 can be assigned to lactones. CO and CO_2 both originated from carboxylic anhydrides. Phenols, ethers, carbonyls, and, consequently, quinones give a CO peak [35]. The TPD measurements performed to our materials are shown in Fig. 3.5.3. The nature of the peaks was detected by MS (Fig. 3.5.4), so the contribution of CO or CO_2 to each TPD profile could be determined. As oxidative treatment became longer, then the amount of oxygen- containing species increased as it is observed in TPD and MS measurements. This fact is in good agreement with the results obtained by elemental analysis. In all cases the amount of CO is much higher than the amount of CO_2. Regarding desorption of CO_2 in AC (black line), a sharp peak assigned to surface carbonates was detected around 160 °C. CO_2 released up to 400 °C is generally related to carboxylic acids, which gave some acidity to the material. The responsible groups of CO_2 eluted at higher temperatures are lactone and anhydride groups. In the case of AC_{3h} and AC_{11h}, CO_2

was also detected, although its contribution to TPD profiles was low. However, two overlapped peaks (product of two contributions: carboxylic acid and lactone) could be observed by making a zoom to the AC_{3h} profile of CO_2 (Fig. 3.5.4-b). The profile of CO_2 corresponding to AC_{11h} showed clearly the contribution of carboxylic acid, while lactone peak became less important. The disappearance of lactone groups may be possible due to their decomposition at 425 °C to a great extent. Zhuang et al. [39] proposed a mechanism for carbon gasification, which may be used to interpret the profiles:

(a) $C_f + O_2 \longrightarrow \text{carbonyls, ethers} \quad (+CO)$

(b) $C_f + O_2 \longrightarrow \text{lactones, anhydrides}$

(c) $C_f + O_2 + \text{carbonyls, ethers} \longrightarrow CO_2 + CO \quad \text{or} \quad \text{carbonyls, ethers}$

(d) $C_f + O_2 + \text{carbonyls, ethers} \longrightarrow \text{lactones, anhydrides}$

(e) $\text{lactones, anhydrides} \longrightarrow CO_2(+CO) + 2C_f$

(f) $\text{carbonyls, ethers} \longrightarrow CO + C_f$

where C_f refers to a free active carbon on the surface. The shoulder at 800 °C - 950 °C (carbonyl, quinone) is clearly higher than the shoulder around 650 °C (phenol, anhydride) in AC and AC_{3h}, which means that (a) prevailed in the oxidation process. As the oxidative treatment was performed for a longer time, then the shoulder due to phenols or/and anhydrides increased, indicating that (d) became

Table 3.5.1

Elemental analyses, surface area and weight loss of all materials

	S_{BET} (m_2/g)	%C	%N	%S	%H	O%	%Ash	%Weight loss
AC	1402	86.42	0.00	1.04	0.15	12.39	7.14	0.00
AC_{3h}	1314	84.08	0.00	0.91	0.10	14.91	5.13	2.47
AC_{11h}	1002	81.17	0.00	0.81	0.13	17.89	6.75	10.27

favoured, possibly because carbonyl-quinone concentration was higher. Thus, the oxidative treatment promoted the increase of quinone, phenol and ether groups. This conclusion is coherent with the FTIR measurements, which also indicated an increase of ether, carbonyl and phenol groups.

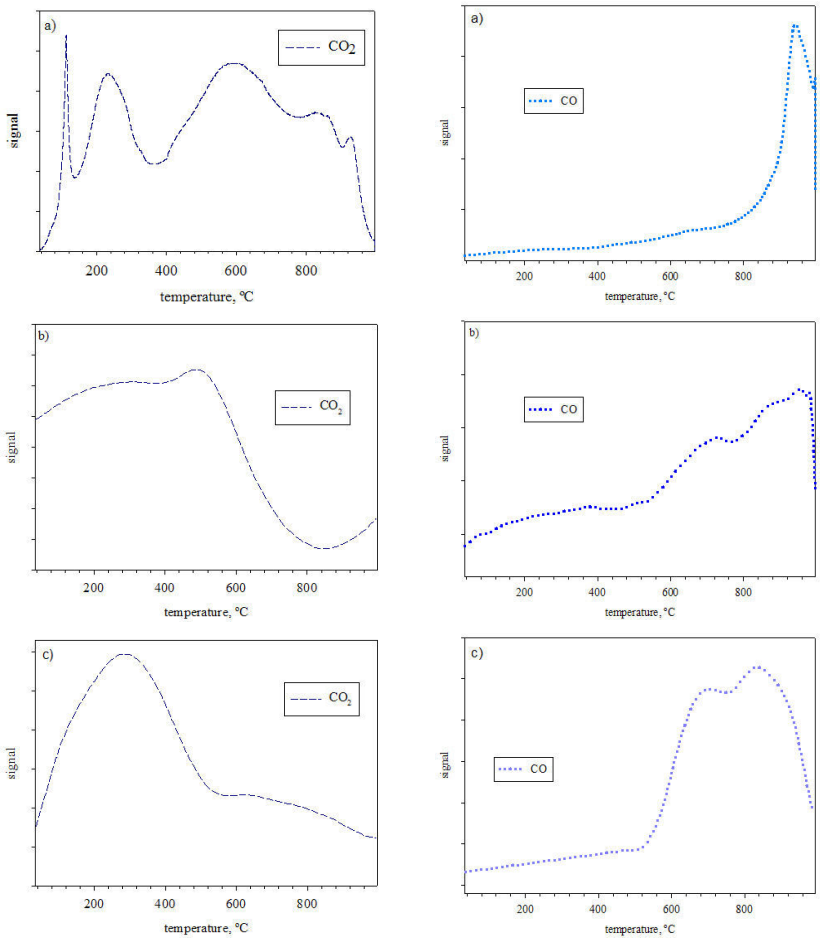

Figure 3.5.4 CO_2 and CO evolutions of: a) original AC; b) AC gasified for 3h, AC_{3h} and c) AC gasified for 11h, AC_{11h}.

The increase of oxygen-containing functionality is consistent with the results of elemental analyses (Table 3.5.1). It is well known that active carbon may have chemically bonded hydrogen [40-43], which is so strongly bonded that it is given off

completely on outgassing at least at 1000 °C [44]. All carbon catalysts released hydrogen after heating up at 996 °C during 30 minutes, which proves the strength of the bonds. Ash content increased slightly for AC_{11h} in comparison to AC_{3h}, probably due to carbon burn-off. As expected, carbon burn-off became higher on longer extent treatments (column weight loss in Table 3.5.1).

The morphology of AC is shown in a typical SEM micrograph in Fig. 3.5.5. Even

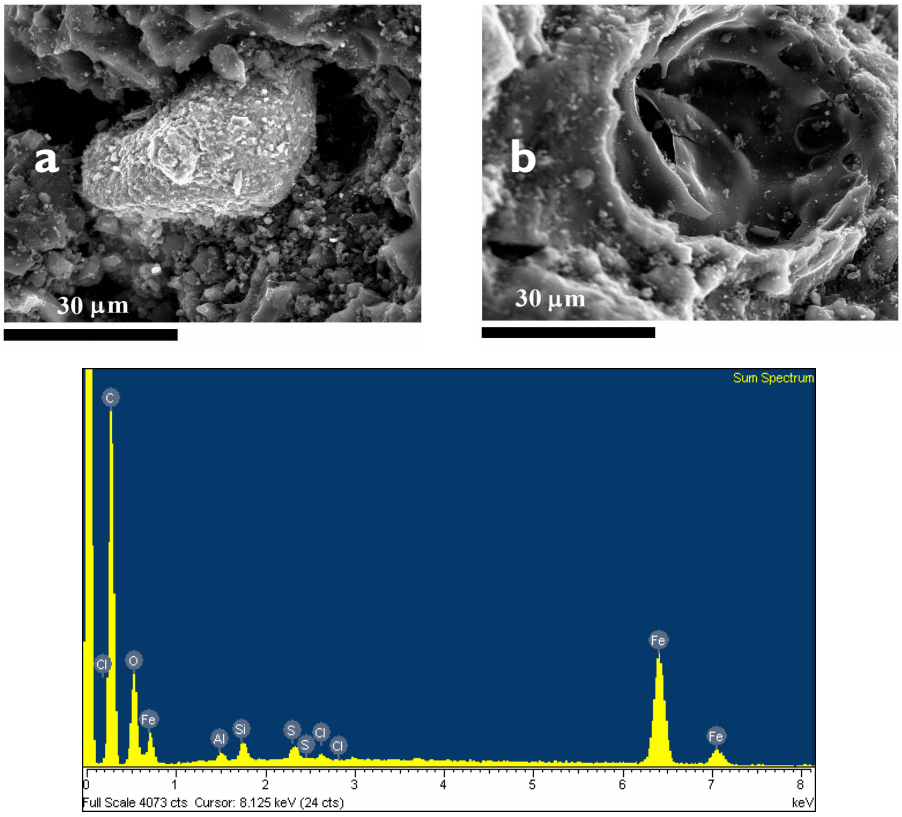

Figure 3.5.5 SEM images and X-ray microanalysis performed to the region represented in a.

though the very small size of its pores makes difficult the study of its microporosity by SEM, this technique is useful to realize the overwhelming number of shapes and sizes of pores. The zero absorption zones in TEM micrograph (Fig. 3.5.6) are identified with porosity. Since the size of these zones is < 2nm, then microporosity

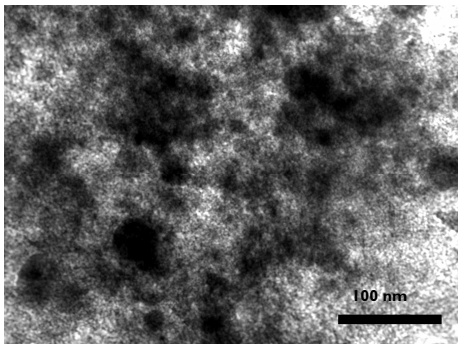

Figure 3.5.6 TEM micrograph of AC.

is present in AC. Microporosity concerns the structure of defective graphene layers, of different dimensions and shapes nearly bonded to each other to create spaces between the graphene layers [45]. XRD microanalysis performed to the image a in Fig. 3.5.5 allowed the determination of a qualitative composition of some salts. Two important elements present in AC were silicon, iron and chloride, as it is shown in the spectrum (Fig. 3.5.5).

Concerning the surface area determined by BET method shown in Table 3.5.1, for higher degrees of oxidation, there is a decrease in the surface area. This fact

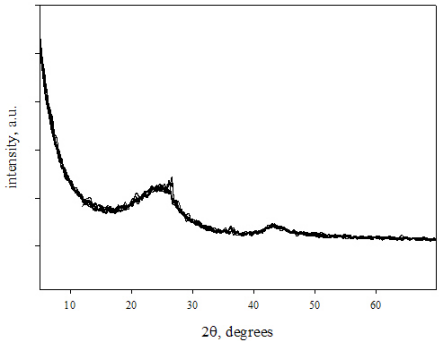

Figure 3.5.7 XRD data of AC.

may be caused by the collapse of the pores during the oxidative treatment. The gas adsorption/desorption isotherm plot of all carbons presented a long nearly flat

branch with a small 'tail' at higher p/p_0 and a narrow hysteresis loop, which may be classified as a type I isotherm in the IUPAC classification [46-48]. This isotherm type is typically exhibited by microporous materials, such as active carbon.

XRD results (Fig 3.5.7) showed two broad peaks based on the diffraction pattern of graphite. Line-broadening is explained as the result of structures made up of associations, roughly parallel, of hydrocarbon (polycyclic) moieties (for the macromolecular structure of coal) and of quite defective, non-planar but roughly parallel associations of carbon atoms, which are the defective micro-graphene layers. Thus, there is no planarity, only strain and defects [45].

3.5.3 Catalytic Activity

Effect of benzene addition

As already commented in the introduction part of this chapter, hydrogenation, using the hydrogen released by the dehydrogenation reaction, became a reaction concomitant with the dehydrogenation reaction. A strategy to minimize the effects of such reaction was the incorporation of a hydrogen capturer. In some cases, the purpose of these patterns is to couple their actions in different ways to achieve

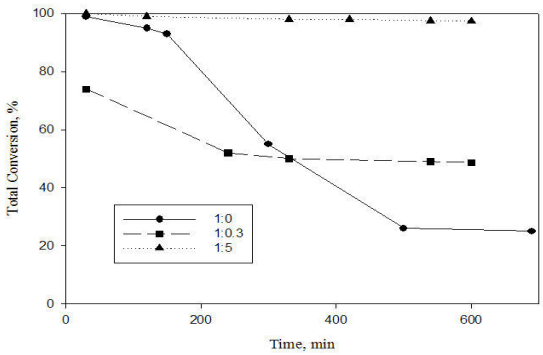

Figure 3.5.8 Total conversion of ethyl linoleate at 240 °C using different amounts of benzene.

certain degree of integration of heat, further shift of thermodynamic equilibrium and simultaneous production of more than one product [49, 50]. Since some preliminary work had been done in our research group concerning the conversion between cyclohexane/benzene, it was thought that benzene could be a suitable capturer. The reaction was performed using different amounts of ethyl linoleate: benzene. The results regarding the total conversion, selectivities towards different products and the influence of benzene on catalytic activity results are shown in the following figures.

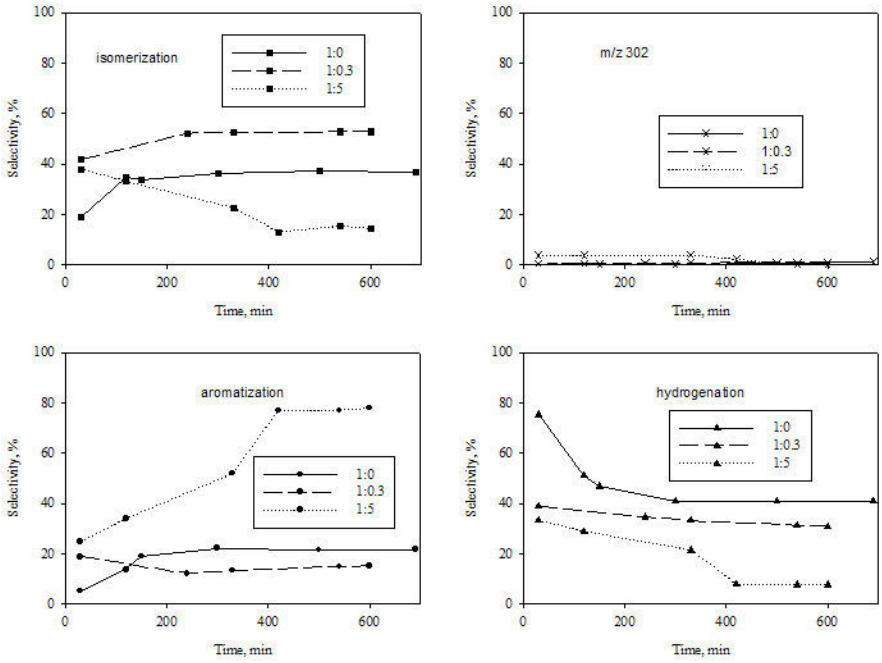

Figure 3.5.9 Selectivity towards different four compound families of ethyl linoleate versus time using different mixtures of ethyl linoleate and benzene.

Total conversions of ethyl linoleate towards different products using benzene as hydrogen capturer are shown in Fig. 3.5.8. When no benzene was being used, a high deactivation of catalyst was detected. The conversion reached values around 100 % at the beginning of the reaction. However, this value became considerably low (around 25%) after 7-8 hours reaction. When using benzene as hydrogen capturer

the catalyst deactivation was controlled. By increasing from zero the amount of benzene used, the deactivation problem appeared to be overcome at certain mixture ratio. For a mixture of ethyl linoleate:benzene 1:5, the total conversion presented constant values along reaction time around 95%. In the case of a mixture ratio of 1:0.3, the achieved conversion was of about 50%, presenting the catalyst a relatively small deactivation. The increase of conversion values and decrease of deactivation as the benzene proportion became higher may be accounted for an improvement of the mass transfer phenomena. The thermodynamic aspects associated to the use of benzene also favoured a higher conversion of ethyl linoleate.

Regarding the selectivity (Fig. 3.5.9-10), four compound families were mainly detected by GC: hydrogenation products such as isomers of ethyl oleate (mono-unsaturated FAEE), aromatization (dehydrogenation) products of aromatic FAEE type, isomerization products which consisted of all ethyl linoleate isomers, that is, all di-unsaturated FAEE, and, finally, a compound family whose mass spectrum presented a molecular peak at m/z 302 (see *Chapter 3.2*), also considered as dehydrogenation products.

On one hand, when the mixture 1:5 was used, the highest conversion (≈95%) and selectivity (≈80%) values towards dehydrogenation products (basically, aromatic FAEE) were obtained. On the other hand, hydrogenation (other than that of benzene to cyclohexane) became less important with values around 10%. Isomerization achieved a selectivity value of about 10%, while m/z 302 was not detected in this case. Isomerization lost importance with time of reaction. Dehydrogenation followed an inverse trend, since it became more important as reaction time went by. This trend was also observed, when using a 1:0.3 mixture. This fact suggests a relation between dehydrogenation (aromatization) and isomerization reactions. Isomerization reaction became the most important reaction showing a selectivity value around 50%. This 1:0.3 mixture gave a hydrogenation selectivity of 30% approximately. In this case, the obtaining of aromatic FAEE had a selectivity value around 15%. The experiments performed without benzene showed low selectivity (21%) towards aromatic FAEE, while the

selectivities to isomerization and hydrogenation products were 37% and 40%, respectively. In all cases, hydrogenation reaction became less important with run time, while isomerization and dehydrogenation reactions did not show a particular trend.

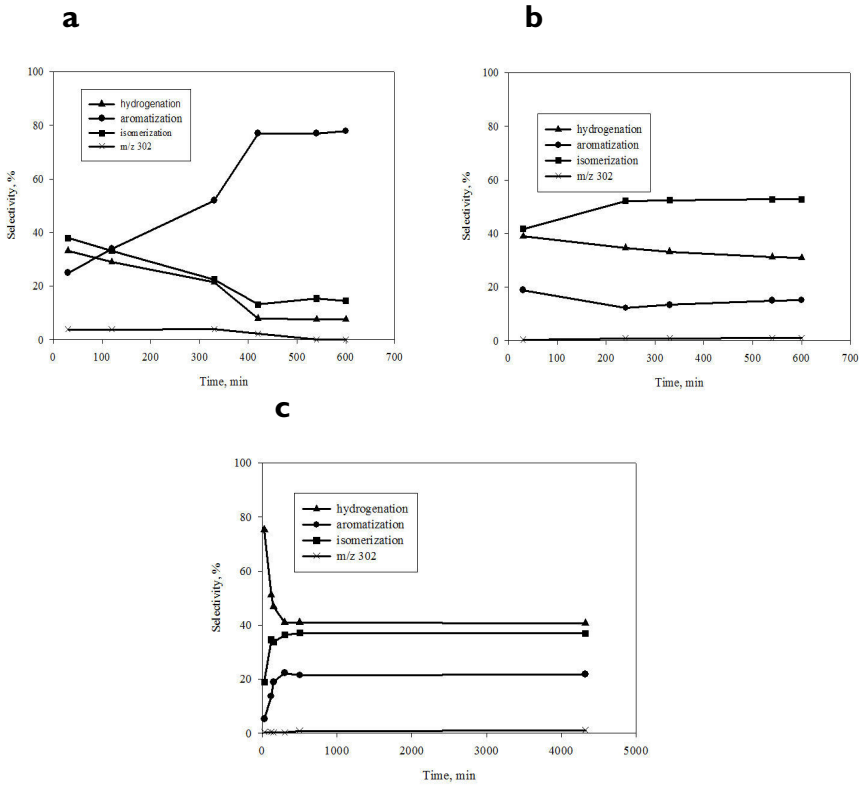

Figure 3.5.10 Selectivity of products versus reaction time using different mixtures of ethyl linoleate and benzene: (a) 1:5, (b) 1:0.3, and (c) 1:0.

Effect of AC gasification

The total conversion (Fig. 3.5.11) did not undergo an important decrease, when the catalyst used had previously been treated under air. In turn, the AC catalyst suffered a deactivation of about 20% in conversion during the first 300 min of reaction. Then, the conversion value remained approximately the same for AC_{3h} and for AC_{11h} and achieved a quite steady value of about 80%, thereafter. Aromatic FAEE were

obtained in the highest proportion (≈38%), when using AC_{11h} as a catalyst. The selectivity towards hydrogenation was around 39%, which represented a decrease in

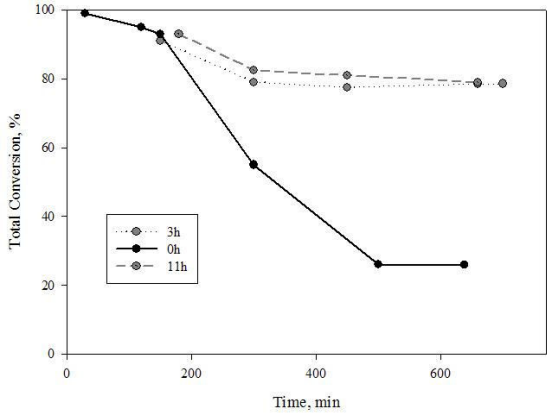

Figure 3.5.11 Total conversion of ethyl linoleate at 240 °C using different oxidized catalysts.

comparison to AC_{0h}, whose hydrogenation selectivity was of 47%. AC_{0h} and AC_{3h} showed similar values of hydrogenation selectivity (≈47%). However, the difference between both lied on the selectivities to aromatic FAEE and isomers of ethyl linoleate. Regarding the obtaining of m/z 302, the selectivity was not higher than 1% in all cases (Fig. 3.5.12).

Definitely, the increase of partially oxidized surface groups on AC had some influence on the dehydrogenation activity, since the obtaining of both aromatic FAEE and compounds with m/z=302 was more important.

When observing the ratio between the selectivities towards hydrogenation and aromatization, in some cases, the hydrogenation value doubles the aromatization value. In those cases the released hydrogen produced by dehydrogenation by ethyl linoleate generates mono-unsaturated FAEE.

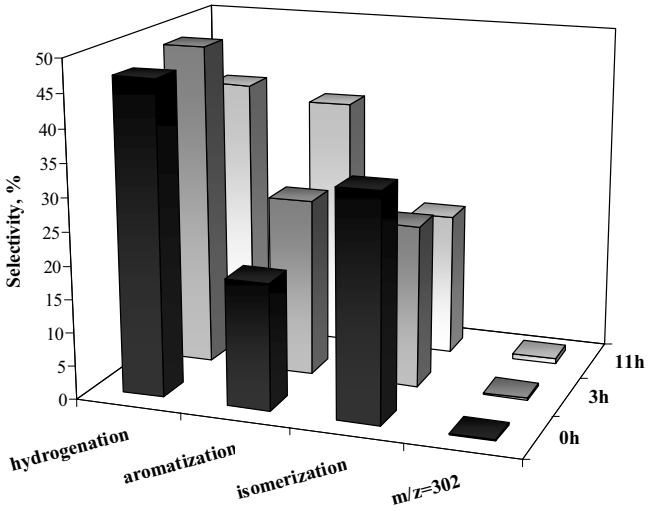

Figure 3.5.12 Selectivity of products after 7h of reaction using different catalysts.

3.5.4 Conclusions

AC presented catalytic activity at 240 °C when being used as a catalyst with ethyl linoleate as starting material in a flow bed reactor under non-oxidative conditions. The four compound families obtained as reaction products were mono-unsaturated FAEE, isomers of FAEE, aromatic FAEE and compounds, whose MS spectra showed a molecular peak of 302.

Benzene acted as a hydrogen capturer giving place to a lower hydrogenation of ethyl linoleate. Moreover, it favoured the total conversion of ethyl linoleate and avoided the deactivation of the catalyst. The mixture of 1:5-ethyl linoleate:benzene turned out to be the optimal for the obtaining of dehydrogenation products.

An oxidative treatment consisting of a thermal treatment under air during 3 or 11 hours modified the surface chemistry of the initial AC. The modification was basically the increment of oxygen-containing functionality, such as quinones, and phenols, which were determined by TPD-MS. The gasification of carbons decreased the surface area of the materials.

The most oxidized carbon, AC_{11h}, turned out to give the highest selectivity towards aromatic FAEE. This activity may be assigned to an increase of functional groups, such as quinone. Those oxidized surface groups did not show deactivation after 300 min run in the presence of hydrogen.

References

[1] B. Behrouzian, P. H. Buist, Curr. Opin. Chem. Biol. 6 (2002) 577.

[2] B. Behrouzian, P. H. Buist, Prostag. Leukotr. Ess. 68 (2003) 107.

[3] E. H. Lee, Catal. Rev. 8 (1973) 285.

[4] M. Muhler, J. Schütze, M. Wesemann, T. Rayment, A. Dent, R. Schlögl, G. Ertl, J. Catal. 126 (1990) 339.

[5] W. P. Addiego, C. A. Estrada, D. W. Goodman, M. P. Rosynek, 146 (1994) 407.

[6] K. Coulter, D. W. Goodman, R. G. Moore, 31 (1995) 1.

[7] W. Weiss, D. Zscherpel, R. Schlögl, 52 (1998) 215.

[8] D. E. Floyd, R. F. Paschke, D. H. Wheeler, W. S. Baldwin, J. Am. Oil Chem. Soc. 33 (1956) 609.

[9] Y. Iwasawa, H. Nobe, S. Ogasawara, J. Catal. 31 (1973) 444.

[10] T. G. Alkhazov, A. E. Lisovskii, Y. A. Ismailov, A. I. Kozharov, Kinet. Catal. 19 (1978) 482.

[11] G. C. Grunewald, R. S. Drago, J. Molec. Catal. 58 (1990) 227.

[12] G. E. Vrieland, P. G. Menon, Appl. Catal. 77 (1991) 1.

[13] R. S. Drago, K. Jurczyk, Appl. Catal. A 112 (1994) 117.

[14] A. Guerrero-Ruiz, I. Rodríguez-Ramos, Carbon 32 (1994) 23.

[15] M. F. R. Pereira, J. J. M. Órfão, J. L. Figueiredo, Appl. Catal. A 184 (1999) 153.

[16] M. F. R. Pereira, J. J. M. Órfão, J. L. Figueiredo, Appl. Catal. A 196 (2000) 43.

[17] M. F. R. Pereira, J. J. M. Órfão, J. L. Figueiredo, Appl. Catal. A 218 (2001) 307.

[18] M. F. R. Pereira, J. J. M. Órfão, J. L. Figueiredo, Carbon 40 (2002) 2393.

[19] M. F. R. Pereira, J. J. M. Órfão, J. L. Figueiredo, Colloids Surf. A 241 (2004) 165.

[20] M. F. R. Pereira, J. J. M. Órfão, J. L. Figueiredo, Carbon 42 (2004) 2807.

[21] N. Maksimova, G. Mestl, R. Schlögl, Stud. Surf. Sci. Catal. 133 (2001) 383.

[22] N. I. Maksimova, V. V. Roddatis, G. Mestl, M. Ledoux, R. Schlögl, Eurasian Chem. Tech. J. 2 (2000) 231.

[23] G. Mestl, N. I. Maksimova, N. Keller, V. V. Roddatis, R. Schlögl, Ang. Chem. Int. Ed. 40 (2001) 2066.

[24] N. Keller, N. I. Maksimova, V. V. Roddatis, M. Schur, G. Mestl, Y. V. Butenko, V. L. Kuznetsov, R. Schlögl, Angew. Chem. Int. Ed. 41 (2002) 1885.

[25] D. S. Su, N. Maksimova, J. J. Delgado, N. Keller, G. Mesta, M. J. Ledoux, R. Schlögl, Catalysis Today 102–103 (2005) 110.

[26] J. A. Maciá-Agulló, D. Cazorla-Amorós, A. Linares-Solano, U. Wild, D. S. Su, R. Schlögl, Catalysis Today 102–103 (2005) 248.

[27] R. C. Bansal, J-B. Donnet, F. Stoeckli, in: Active Carbon, Marcel Dekker, Inc., New York, 1988. ISBN 0-8427-7842-1

[28] P. E. Fanning, M. A. Vannice, Carbon 31 (1993) 721.

[29] E. Papier, E. Guyon, N. Perol, Carbon 16 (1978) 133.

[30] F. Rositani, A. L. Antonncci, M. Minutoli, N. Giorclane, A. Villari, Carbon 25 (1987) 325.

[31] Bhabendra K. Pradhan, N. K. Sandle, Carbon 37 (1999) 1323.

[32] A. Dandekar, R. T. K. Baker, M. A. Vannice, Carbon 36 (1998) 1821.

[33] G. Socrates, in: Infrared Characteristic Group Frequencies, Wiley, Chichester, 1980. ISBN 0-471-27592-1

[34] J. Guo, A. C. Lua, J. Therm. Anal. Cal. 60 (2000) 417.

[35] J. L. Figueiredo, M. F. R. Pereira, M. M. A. Freitas, J. J. M. Órfão, Carbon 37 (1999) 1379.

[36] J. L. Falconer, J. A. Schwarz, Catal. Rev-Sci. Eng. 25 (1983) 141.

[37] H. P. Boehm, G. Bewer, in: Proc. 4th London Carbon and Graphite Conf., London, UK, 1974, p. 344.

[38] H. P. Boehm, Carbon, 32 (1994) 759.

[39] Q. L. Zhuang, T. Kyotany, A. Tomita, Ener. Fuels 9 (1995) 630.

[40] B. R. Puri, B. C. Bansal, 1 (1964) 451.

[41] R. C. Bansal, T. L. Dhami, S. Parkash, 15 (1977) 157.

[42] M. L. Studebaker, Rubber Chem. Technol. 30 (1957) 1400.

[43] J. P. Redmond, P. L. Walker, Jr., J. Phys,. Chem. 64 (1960) 1093.

[44] B. R. Puri, R. C. Bansal, Chem. Ind. London, 574 (1963).

[45] H. Marsh, F. Rodríguez-Reinoso, in: Activated Carbon, Elsevier Ltd., Oxford, 2006. ISBN 0-08-044463-6

[46] I.U.P.A.C "Definitions, terminology and Symbols in Colloid and Surface Chemistry", part. I of Appendix II, (D. H. Everett) Pure Appl. Chem. 31 (1972) 579.

[47] I.U.P.A.C "Terminology in Heterogeneous Catalysis", part. II of Appendix II, (R. L. Burwell, Jr.) Pure Appl. Chem. 45 (1976) 71.

[48] K.S.W. Sing, D.H. Everett, R.A.W. Haul, L. Moscou, R.A. Pietotti, J. Rouquerol and T. Siemienieska, Pure Appl. Chem. 57 (1985) 603.

[49] E. Gobina, K. Hou, R. Hughes, Chem. Eng. Sci. 50 (1995) 2311.

[50] M. E. E. Abashar, A. A. Al-Rabiah, Chem. Eng. Process. 44 (2005) 1188.